

#### TẠP CHÍ KHOA HỌC TRƯỜNG ĐẠI HỌC SỬ PHẠM TP HỒ CHÍ MINH

HO CHI MINH CITY UNIVERSITY OF EDUCATION
JOURNAL OF SCIENCE

Vol. 22, No. 9 (2025): 1542-1553

ISSN: 2734-9918 Tập 22, Số 9 (2025): 1542-1553 Website: https://journal.hcmue.edu.vn

https://doi.org/10.54607/hcmue.js.22.9.4271(2025)

Research Article

# SIMULATING MOLECULAR NONADIABATIC ALIGNMENT

Bui Van Nguyen<sup>1</sup>, Hoang Trong Dai Duong<sup>1,2</sup>, Tran Phuc Khang<sup>3</sup>, Trieu Doan An<sup>1</sup>, Phan Thi Ngoc Loan<sup>1</sup>

<sup>1</sup>Ho Chi Minh City University of Education, Vietnam

<sup>2</sup>Nuclear Training Center - Vietnam Atomic Energy Institute, Hanoi, Vietnam

<sup>3</sup>New Jersey Institute of Technology, Newark, United States

\*Corresponding author: Hoang Trong Dai Duong – Email: hoangtrongdaiduong00@gmail.com
Received: May 13, 2024; Revised: February 14, 2025; Accepted: February 19, 2025

#### **ABSTRACT**

Recently, molecular alignment techniques have become an appealing topic in molecular and optical physics, strong-field physics, femtosecond chemistry, and attosecond physics. Despite the availability of several alignment techniques, molecular nonadiabatic alignment is widely used in both theoretical and experimental studies due to assembling molecules in space for a sufficiently short period of time under field-free conditions, avoiding the laser's effect on the interested physical or chemical phenomena. As a result, developing a program that simulates molecular nonadiabatic alignment is necessary to ensure that numerical results match experimental observations. Existing tools, such as those by Oppermann et al. (2012) and Sonoda et al. (2018), are either limited to specific molecules or require significant modifications for alignment simulations. For that reason, we provide a program that simulates linear-molecular nonadiabatic alignment. In this paper, we present the numerical simulation of the time evolution of a molecular rotational wave packet by solving the time-dependent Schrödinger equation and evaluate our results with reliable published studies. Additionally, a challenge in such simulations is determining the optimal value of the expansion used for numerical simulation. We provide a systematic method for selecting the optimal parameter  $J_{max}$ , ensuring both computational efficiency and solution convergence. The program is evaluated for  $N_2$ ,  $CO_2$  and OCS with a variety of laser pulses and rotational temperature. Program available at: https://github.com/DuongDHoangTrong/HCMUE\_Alignment.

*Keywords:* laser-matter interaction; linear molecules; molecular nonadiabatic alignment; rotational wave packet

#### 1. Introduction

In recent decades, laser-matter interaction has attracted the attention of the community studying strong field physics and attosecond science. When atoms or molecules are exposed to an intense and femtosecond pulse, a variety of high-order nonlinear effects occur,

Cite this article as: Bui, V. N., Hoang, T. D. D., Tran, P. K., Trieu, D. A., & Phan, T. N. L. (2025). Simulating molecular nonadiabatic alignment. Ho Chi Minh City University of Education Journal of Science, 22(9), 1542-1553. https://doi.org/10.54607/hcmue.js.22.9.4271(2025)

including high-order harmonic generation (Burnett et al., 1977), above-threshold ionization (Bashkansky et al., 1988; Eberly et al., 1991), and nonsequential double ionization (Watson et al., 1997). These nonlinear phenomena allow for imaging molecules and probing molecular dynamics (Itatani et al., 2004; Qin & Zhu, 2017). In those phenomena, the angle between the molecular axis and the laser polarization significantly impacts laser-matter interaction. The reason is that if the molecular ensemble—is isotropically distributed, the observations of related phenomena are averaged, leading to missing information about—the angular distribution of the molecule. This dragged the interest in molecular alignment techniques within the field of ultrafast molecular imaging (Cocker et al., 2016), attosecond science (Villeneuve, 2018), and surface science (Seideman, 1997). Consequently,—several efforts have been made to develop molecular alignment techniques (Burnett et al., 1977; Physikd et al., 1991; Pullman et al., 1990; Sinha et al., 1974; Stapelfeldt & Seideman, 2003)

Among the various molecular alignment techniques, those based on a strong nonresonant linearly polarized laser field are most versatile (Friedrich & Herschbach, 1995; Seideman, 1995). When a molecule interacts with an intense laser pulse, an induced dipole is created due to its anisotropic polarization. Consequently, torque is produced on the axis of the molecules, forcing them to align with the direction of laser polarization (Torres et al., 2005).

In the temporal domain of laser duration, two distinct regimes can be identified: adiabatic alignment and nonadiabatic alignment (Omiste et al., 2011; Seideman & Hamilton, 2005; Torres et al., 2005). In the case of nonadiabatic alignment, the laser pulse with its duration less than the characteristic molecular rotational time is used. When a molecular ensemble interacts with this ultrashort laser pulse, a rotational wave packet is created. This wave packet is a coherent superposition of the rotational states that phase and diphase over time. This leads to the phenomenon known as 'revival', wherein a molecular sample can restore a state of high degree of alignment in the absence of the laser field (free field) (Jin et al., 2010).

With the ability to achieve field-free alignment, nonadiabatic alignment is the most preferred technique (Omiste et al., 2011) and has been studied in a number of experimental (Oppermann et al., 2012) and theoretical papers (Jin et al., 2010; Omiste et al., 2011). For on molecular alignment can be divided into two categories: the effects of decades, work temperature or laser settings on alignment (Cocker et al., 2016; Yang & Zhou, 2006) and the impacts of alignment on other nonlinear processes (Jin et al., 2020; Jiang et al., 2022). The majority of these studies focus on a limited number of nonpolar molecules (N<sub>2</sub>, O<sub>2</sub>, I<sub>2</sub>, CO<sub>2</sub>, CS<sub>2</sub>) (Péronne et al., 2004; Yang & Zhou, 2006; Jin et al., 2010; Pickering et al., 2018), and (Loriot et al., 2007). Despite several publications, there is a scarcity rarely on polar molecules of publicly available software that simulates the alignment process. This work (Oppermann et al., 2012) offers a software for nonpolar molecules; its applicability is limited to a select few targets. Another accessible code that can handle user-defined molecular parameters is specifically designed to simulate the orientation process for polar molecules only (Sonoda et al., 2018).

In this paper, we present a program that simulates the molecular alignment process. Unlike existing tools (Oppermann et al., 2012; Sonoda et al., 2018), our program is unique in its ability to handle user-defined molecular parameters for nonpolar and especially polar molecules, a capability not available in other software. It achieves this by numerically solving the time-dependent Schrödinger equation, which yields the temporal evolution of a molecular rotational wave packet.

Moreover, a major challenge in achieving a convergent solution is selecting the maximum rotational quantum number  $J_{max}$ , which determines the number of rotational states included in the calculations. Choosing an appropriate method is crucial for balancing computational efficiency and accuracy. An overly small  $J_{max}$  leads to non-convergent results, while an unnecessarily large value increases computational costs without improving accuracy. Despite its significance,  $J_{max}$  is often determined empirically in prior studies, leaving room for improvement through a systematic approach. To address this, we propose a method for determining the optimal  $J_{max}$  based on the Boltzmann distribution of rotational states, which ensures reliable convergence while minimizing computational effort.

The rest of this paper is structured as follows. Firstly, we present the theoretical backgrounds of the molecular alignment process. Second, we examine the convergence tendency of our code's solutions and introduce a method for determining the optimal  $J_{max}$  based on the Boltzmann distribution of rotational states. Finally, we assess the reliability of our program through comparison with recent research.

# 2. Theoretical model and computation method

# 2.1. Evolution of rotational wave packet

We consider linear molecules exposed to a non-resonant linearly polarized laser field.

$$\vec{E}(t) = \vec{e}E_0 f(t) \cos \cos \omega t$$
, #(1)

where  $\vec{e}$  is a unit vector along the polarization direction,  $E_0$  is the field amplitude,  $\omega$  is the laser frequency, and f(t) is the pulse envelope whose temporal profiles are given by a Gaussian function

$$f(t) = \exp \exp \left(-2 \ln \ln 2 \, \frac{t^2}{\tau^2}\right), \#(2)$$

where  $\tau$  is the pulse duration.

When this ultrashort laser pulse interacts with a molecular ensemble, it excites a coherent superposition of rotational states, also called a rotational wave packet, in each molecule. Under the rigid rotor approximation, the rotational wave packet is governed by TDSE with the Hamiltonian (Yang & Zhou, 2006), which is expressed in atomic units by

$$\widehat{H} = B\widehat{J}^2 + \widehat{H}_{polar}, \#(3)$$

where B is the rotational constant of the molecule,  $\hat{J}$  is the angular momentum operator, and  $\hat{H}_{polar}$  represents the polarizability interaction term averaged over the laser cycle (Péronne

et al., 2004; Seideman & Hamilton, 2005), is written as

$$\widehat{H}_{polar} = -\frac{1}{4} \Delta \alpha E_0^2 f^2(t) \theta , \#(4)$$

where  $\Delta \alpha = \alpha_{\parallel} - \alpha_{\perp}$  is polarizability anisotropy, which represents the differences between the polarizabilities parallel  $(\alpha_{\parallel})$  and perpendicular  $(\alpha_{\perp})$  to the molecular axis, and  $\theta$  is the angle between the molecular axis and the electric field vector.

The TDSE is to be solved numerically using the split-operator technique (Tong & Chu, 1997, 2000). The wave packet, solution of TDSE (Péronne et al., 2004), can be expanded in the rotational state basis as

$$|\Psi(\theta,t)\rangle = \sum_{I,M} C_{J,M}(t)|JM\rangle, \#(5)$$

where  $C_{J,M}(t)$  is the expansion coefficient and  $|JM\rangle$  is the rotational states represented in space by the spherical harmonics  $Y_J^M(\theta, \phi)$ . After turning off the laser pulse at  $t = \tau_{laser}$ , the wave packet propagates in the free field (Jin et al., 2010), and can be calculated simply as

$$|\Psi(\theta,t)\rangle = \sum_{J,M} C_{J,M}(\theta,t=\tau_{laser})e^{-BJ(J+1)t}|JM\rangle.\#(6)$$

#### 2.2. Degree of alignment

Initially, a molecular sample can be assumed to be a thermal ensemble characterized by a temperature T, with the population of its states,  $|JM\rangle$ , following the Boltzmann distribution function (Torres et al., 2005)

$$\Gamma_{JM}(T) = \frac{1}{Z(T)} \exp \exp \left[ -\frac{BJ(J+1)}{k_B T} \right] , \#(7)$$

where  $k_B$  is the Boltzmann constant, and Z(T) is the partition function. The above function is valid for heteronuclear molecules only. For homonuclear diatomic molecules, the factor  $g_s$  arises from the nuclear spin statistics , and gives a distinct weight to states of different J parity (e.g.,  $N_2$  has  $g_s^{Jodd} = 1$  and  $g_s^{Jeven} = 2$ ) (Torres et al., 2005):

$$\Gamma_{JM}(T) = \frac{g_s}{Z(T)} \exp \exp \left[ -\frac{BJ(J+1)}{k_B T} \right] . \#(8)$$

This is why programs designed for homonuclear molecules cannot be used for heteronuclear molecules without adding  $g_s$  to the source code.

The degree of alignment of a molecular sample can be determined by the expectation value of  $\theta$  (Péronne et al., 2004; Jin et al., 2010; Oppermann et al., 2012), written as

$$\langle \theta \rangle (t) = \sum_{IM} \Gamma_{JM}(T) \langle \Psi_{JM}(\theta, t) \rangle. \#(9)$$

This value ranges from 0, where all molecules are anti-aligned in a plane perpendicular to the laser polarization axis, to 1, where all molecules are aligned precisely along that axis,

and isotropic media have this value equal to 1/3.

# 2.3. Numerical method

Our numerical calculations follow a specific workflow, as shown in Fig. 1. This procedure contains two steps: *laser field* and *field-free*. The details of each step are presented below.

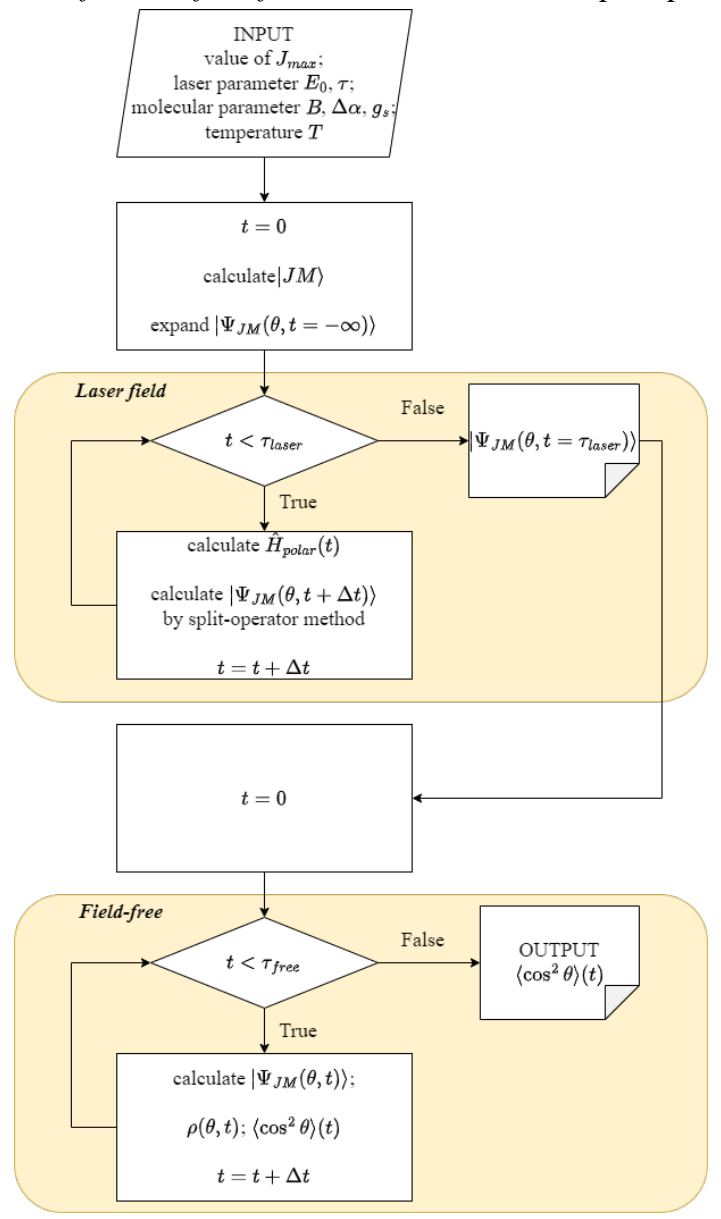


Figure 1. The workflow of our program

# 2.3.1. Laser field

In the *laser field* steps, the initial wave function  $|\Psi(\theta, t = -\infty)\rangle$  is evolved under the laser field with an interval  $\tau_{laser}$ . To propagate the wave function from t to  $t + \Delta t$ , we expand the rotational wave function into a combination of spherical harmonic functions as shown in Eq. (5), and solve TDSE with the split-operator technique (Bandrauk & Shen, 1993), written as

$$\begin{split} |\Psi_{JM}(\theta,t+\Delta t)\rangle \\ \approx &exp\ exp\ \left[-i\frac{B\hat{J}^2\Delta t}{2}\right]\ exp\ exp\ \left[-i\widehat{H}_{polar}(t)\Delta t\right] \\ &exp\ exp\ \left[-i\frac{B\hat{J}^2\Delta t}{2}\right]\ |\Psi(\theta,t)\rangle.\#(10) \end{split}$$

Equation (9) shows that the time propagation is achieved by three steps

- (i) Applying  $exp\ exp\ \left[-i\frac{B\hat{J}^2\Delta t}{2}\right]$  on  $|\Psi_{JM}(\theta,t)\rangle$  to transform it into the energy space and propagate for half a time step, we receive  $|\Psi^{(i)}(\theta,t)\rangle$ ,
- (ii) Applying  $exp\ exp\ \left[-i\widehat{H}_{polar}(t)\Delta t\right]$  on  $|\Psi^{(i)}(\theta,t)\rangle$  to transform it into coordinate space and propagate for a time step, we receive  $|\Psi^{(ii)}(\theta,t)\rangle$ ,
- (iii) Applying  $exp\ exp\ \left[-i\frac{B\hat{J}^2\Delta t}{2}\right]$  on  $|\Psi^{(ii)}(\theta,t)\rangle$  to transform it back into the energy space and propagate for half a time step, we receive  $|\Psi^{(iii)}(\theta,t)\rangle$  which is  $|\Psi_{IM}(\theta,t+\Delta t)\rangle$ .

This propagation of the wavefunction is accomplished until the laser is turned off. At the end of the step, we obtain the wave function  $|\Psi_{JM}(t=\tau_{laser})\rangle$ .

# 2.3.2. Field-free

In the field-free step, the wave function when the laser is turned off  $|\Psi_{JM}(t=\tau_{laser})\rangle$  is propagated under the free field with an interval  $\tau_{free}$ . The wave function at the specific moment t is simply calculated as shown in Eq. (6). Then, we compute the time-dependent alignment distribution at a given temperature T (Jiang et al., 2022), which can be obtained as

$$\rho(\theta,t) = \sum_{JM} \Gamma_{JM}(T) |\Psi_{JM}(\theta,t)|^2. \#(11)$$

Our program provides the angular distribution since it enables users to calculate other physics quantities. Finally, we measure the degree of alignment alternatively (Jiang et al., 2022), followed by

$$\langle \theta \rangle (t) = 2\pi \int_{0}^{\pi} \rho(\theta, t) \sin \sin \theta \ d\theta. \#(12)$$

# 3. Results and discussion

# 3.1. Results of the alignment degree and its convergence

In principle, solving TDSE requires representing the wavefunction in Eq. (5) with an infinite number of basis states  $|JM\rangle$ . However, in practice, numerical methods can only handle a finite number of basis states  $|JM\rangle$ . With a sufficient number of states, the solution obtained numerically converges to the exact solution. In the previous source code, the number of states  $J_{max}$  is chosen based on experience. In this Section, we examine the optimal number of states,  $J_{max}$  based on Boltzmann's distribution, for an ensemble of  $N_2$  molecules at a variety of temperatures when it is exposed to a laser pulse of 60 fs duration and  $2 \times 10^{13} \ W/cm^2$  peak intensity. Table 1 represents molecular parameters of  $N_2$ .

Molecule	B (cm <sup>-1</sup> )	$\Delta \alpha \left( \mathring{A}^3 \right)$	$\mathbf{g}_{\mathrm{s}}^{\mathrm{J}_{\mathrm{odd}}}$	$\mathbf{g}_{\mathrm{s}}^{J_{\mathrm{even}}}$
$N_2$	1.9896	0.93	1	2
$CO_2$	0.3913	2.10	1	0
OCS	0.2029	4.04	1	1

**Table 1.** Molecular parameters used in the calculations

To determine the optimal value of  $J_{max}$ , we need to examine the Boltzmann distribution, which yields the population of each rotational state  $|J\rangle$  at a variety of temperatures. Fig. 2 shows that when the temperature rises , the probability of occupying the high rotational state increases significantly. In this case, arising of the contribution of high rotational states requires a greater value of  $J_{max}$  for converged solutions. Any state with a population smaller than  $\varepsilon = 1 \times 10^{-5}$  is assumed not to contribute to the wave packet. Based on Fig. 2, we examine different values of  $J_{max}$  around 8, 12, and 17, the rotational quantum numbers beyond which state populations become negligible, at the temperatures of  $T = 20 \, K$ , 50 K and 100 K, respectively.

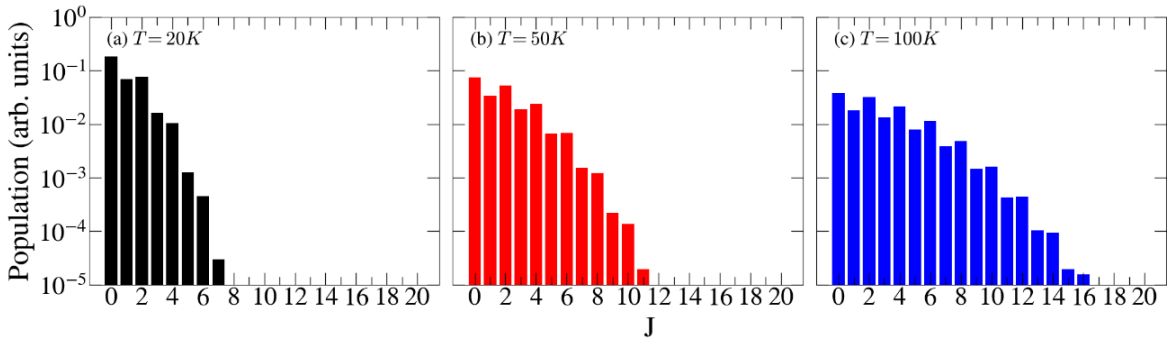


Figure 2. The thermal population of molecular rotational states at different temperatures for  $N_2$ 

In order to examine whether the above estimate  $J_{max}$  is enough for ensuring the degree, we continue to simulate the process convergence for simulating the alignment with  $J_{max}$  values below and higher than that estimated value. In Fig. 3, we show the degree of alignment for  $N_2$  at different temperatures as a function of time when using values of  $J_{max}$ in which state its population starts to vanish and around that state. Note that the  $\sim$ 8.6 ps and half-time revival ~4.3 ps. Near these revivals, the molecular time alignment changes significantly from an isotropic distribution  $\langle \theta \rangle \sim 1/3$  into a peak or dip of the graph, as seen in all cases. The solutions, whether convergent or not, capture the line tendency of degree of alignment; and yield precisely the maxima (aligned molecules) and minima (anti-aligned molecules), which are near 4.1 ps, 8.6 ps; and 4.3 ps, 8.3 ps, respectively. Furthermore, for a given temperature, the values of the maxima and minima are the same for any value of  $J_{max}$ . Those points consistently reinforce the convergence of solutions.

Moreover, it is crucial to ensure that the chosen  $J_{max}$  value adequately represents the

rotational states contributing to the molecular wave packet while minimizing unnecessary computational expense. Our recommended approach is to set  $J_{max}$  to the rotational state where the population, based on the Boltzmann distribution, becomes negligibly small (e.g., below a threshold such as  $\varepsilon = 1 \times 10^{-5}$ ). At this point, higher rotational states have minimal impact on the wave packet and can be excluded from calculations. In our example, at 20 K, 50 K, and 100 K, the optimal values  $J_{max}$  were found to be 8, 12, and 17, respectively, as higher states had insignificant contributions. In contrast, using a value lower than the optimal one results in non-convergent solutions, particularly at low temperatures, whereas solutions with values higher than the optimal show no significant difference compared to the optimal value. This method ensures that the numerical solutions are both convergent and computationally efficient.

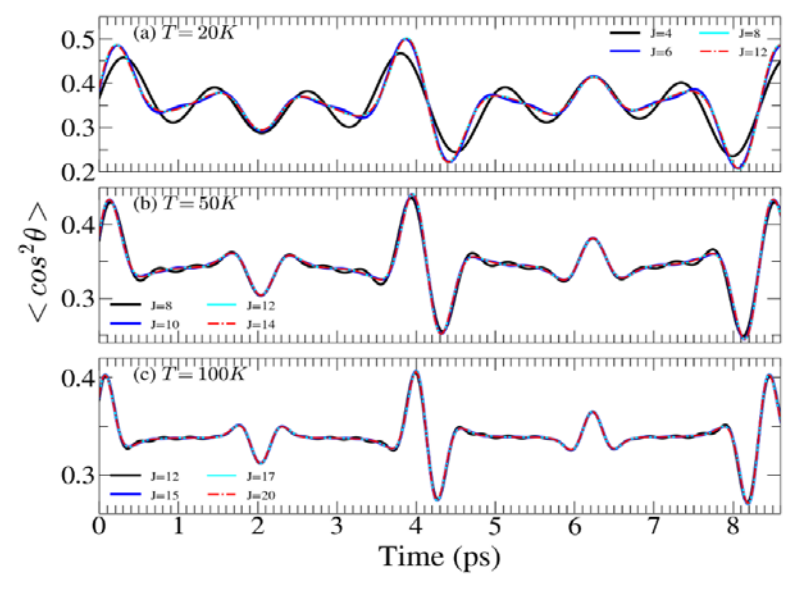


Figure 3. Degree of alignment by time when exposed  $N_2$  molecules to a laser pulse of 60 fs duration and  $2 \times 10^{13}$  W/cm<sup>2</sup> peak intensity at different temperatures. The cyan lines represent results obtained using the estimated value of  $J_{max}$  in which state that its population start to vanish. The black and blue lines (red lines), on the other hand, show the results of calculations with values of  $J_{max}$  that are smaller (larger) than the above value, respectively. The red and cyan lines match each other, demonstrating that these solutions are converged. In contrast, the black and blue lines are different from the others, showing these solutions are unconverged. From case (a) to case (c) rate of convergence increases rapidly

#### 3.2. The reliability of the solutions

This section demonstrates the reliability of our solutions, including both polar and nonpolar molecules, by comparing them to other works. Table 1 displays the molecular parameters considered in our analysis. Note that all the results presented here have reached convergence. Below, we first present the molecular information and the laser pulse used for adiabatic alignment. Besides, the experimental temperature is also addressed. Then, we summarize the results of the

alignment degree, and benchmarking them with those published before.

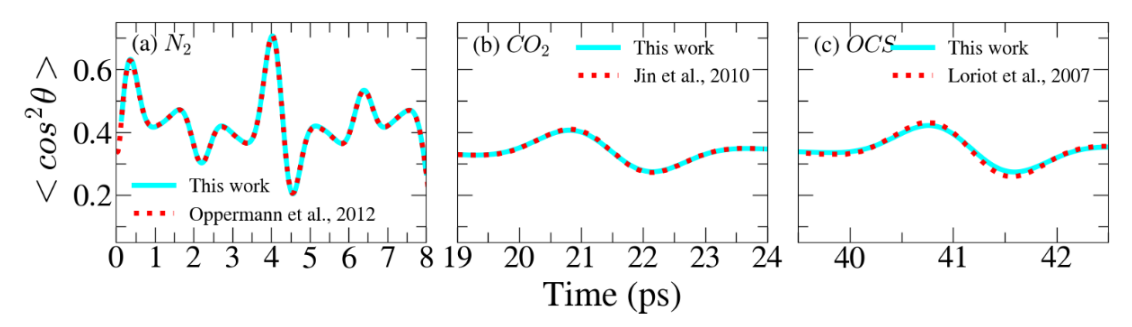


Figure 4. Comparison between our solutions (cyan lines) and other works (red lines) (Oppermann et al., 2012; Jin et al., 2010; Loriot et al., 2007), respectively. A variety of lasers pulses and rotational temperatures are concerned. The molecules used follow as (a)  $N_2$ ; (b)  $CO_2$ ; and (c) OCS

# 3.2.1. Nonpolar homoatomic molecule

First, we verify our code's reliability with a simple molecule  $N_2$ . Here, we compare our results with Oppermann et al. ( 2012). Figure 4. (a) displays both results. 790 nm pump pulse with a 70 fs duration and the peak intensity of In this work, a  $3 \times 10^{13} W/cm^2$  is used, and the rotational temperature is 20 K.

#### 3.2.2. Nonpolar heteroatomic molecule

For this case, we specifically chose the molecule  $CO_2$  to verify our code's capacity to handle molecules with either only odd or only even  $g_s$  is preset. We compared our results to a 790 nm pump pulse with a 140 fs duration the study (Jin et al., 2010), which utilizes peak intensity of 4.5  $\times$  10<sup>13</sup>  $W/cm^2$ , and the rotational temperature is 25 K. Figure 4. (b) shows the comparison of these results.

# 3.2.3. Polar molecule

Finally, we validated our code against the molecular-alignment study of the polar molecule OCS by Loriot et al. (2007). That experiment used a 790 nm pump pulse with 70 fs duration, a peak intensity of  $2 \times 10^{13} W/cm^2$ , and a rotational temperature is 100 K. Figure 4. (c) shows the comparison between our results and those reported in that study.

# *3.2.4. Summary*

Fig. 4 demonstrates a close match between our simulation results and those from previous studies (Jin et al., 2010; Loriot et al., 2007; Oppermann et al., 2012). Overall, our program demonstrates a high level of agreement with previous works. Notably, for the OCS molecule, the maxima and minima of the degree of alignment differ slightly. However, the timing of these extrema remains consistent with the reference work (Loriot et al., 2007). Furthermore, the employment of laser pulses with varied characteristics and rotational temperatures throughout the comparisons demonstrates the versatility and suitability of our program for a wide range of scenarios.

#### 4. Conclusion and outlook

This work presents a reliable program for simulating the molecular alignment of both

polar and non-polar molecules. Its reliability has been thoroughly validated through comparisons with established research. This versatile tool enables researchers to provide consistent results in simulation studies. Based on the fundamentals of molecular alignment, we plan to build a source code that simulates molecular orientation. Additionally, we highlight an effective approach for selecting  $J_{max}$  to ensure a good rate of convergence, based on the thermal population of molecular rotational states.

- **Conflict of Interest:** Authors have no conflict of interest to declare.
- ❖ Acknowledgement: This work was funded by Vingroup and supported by Vingroup Innovation Foundation (VINIF) under project code VINIF.2021.DA00031.

#### **REFERENCES**

- Bandrauk, A. D., & Shen, H. (1993). Exponential split operator methods for solving coupled time-dependent Schrödinger equations. *The Journal of Chemical Physics*, 99(2), 1185-1193. https://doi.org/10.1063/1.465362
- Bashkansky, M., Bucksbaum, P. H., & Schumacher, D. W. (1988). Asymmetries in above-threshold ionization. *Physical Review Letters*, 60(24), 2458-2461. https://doi.org/10.1103/PhysRevLett.60.2458
- Burnett, N. H., Baldis, H. A., Richardson, M. C., & Enright, G. D. (1977). Harmonic generation in CO2 laser target interaction. *Applied Physics Letters*, 31(3), 172-174. https://doi.org/10.1063/1.89628
- Cocker, T. L., Peller, D., Yu, P., Repp, J., & Huber, R. (2016). Tracking the ultrafast motion of a single molecule by femtosecond orbital imaging. *Nature*, *539*(7628), 263-267. https://doi.org/10.1038/nature19816
- Eberly, J. H., Javanainen, J., & Rzązewski, K. (1991). Above-threshold ionization. *Physics Reports*, 204(5), 331-383. https://doi.org/10.1016/0370-1573(91)90131-5
- Friedrich, B., & Herschbach, D. (1995). Alignment and trapping of molecules in intense laser fields. *Physical Review Letters*, 74(23), 4623-4626. https://doi.org/10.1103/PhysRevLett.74.4623
- Itatani, J., Lavesque, J., Zeidler, D., Niikura, H., Pépin, H., Kieffer, J. C., Corkum, P. B., & Villeneuve, D. M. (2004). Tomographic imaging of molecular orbitals. *Nature*, 432(7019), 867-871. https://doi.org/10.1038/nature03183
- Jiang, C., Jiang, H., Chen, Y., Li, B., Lin, C. D., & Jin, C. (2022). Genetic-algorithm retrieval of the molecular alignment distribution with high-order harmonics generated from transiently aligned CO2 molecules. *Physical Review A*, 105(2). https://doi.org/10.1103/PhysRevA.105.023111
- Jin, C., Le, A. T., Zhao, S. F., Lucchese, R. R., & Lin, C. D. (2010). Theoretical study of photoelectron angular distributions in single-photon ionization of aligned N2 and CO2. *Physical Review A Atomic, Molecular, and Optical Physics*, 81(3), 1-12. https://doi.org/10.1103/PhysRevA.81.033421
- Jin, C., Wang, S. J., Zhao, X., Zhao, S. F., & Lin, C. D. (2020). Shaping attosecond pulses by controlling the minima in high-order harmonic generation through alignment of CO2 molecules. *Physical Review A*, 101(1), 1-12. https://doi.org/10.1103/PhysRevA.101.013429

- Loriot, V., Tzallas, P., Benis, E. P., Hertz, E., Lavorel, B., Charalambidis, D., & Faucher, O. (2007). Laser-induced field-free alignment of the OCS molecule. *Journal of Physics B: Atomic, Molecular and Optical Physics*, 40(12), 2503-2510. https://doi.org/10.1088/0953-4075/40/12/023
- Omiste, J. J., Gärttner, M., Schmelcher, P., González-Férez, R., Holmegaard, L., Nielsen, J. H., Stapelfeldt, H., & Küpper, J. (2011). Theoretical description of adiabatic laser alignment and mixed-field orientation: The need for a non-adiabatic model. *Physical Chemistry Chemical Physics*, *13*(42), 18815-18824. https://doi.org/10.1039/c1cp21195a
- Oppermann, M., Weber, S. J., & Marangos, J. P. (2012). Characterising and optimising impulsive molecular alignment in mixed gas samples. *Physical Chemistry Chemical Physics*, *14*(27), 9785-9791. https://doi.org/10.1039/c2cp40677b
- Péronne, E., Poulsen, M. D., Stapelfeldt, H., Bisgaard, C. Z., Hamilton, E., & Seideman, T. (2004). Nonadiabatic laser-induced alignment of iodobenzene molecules. *Physical Review A Atomic, Molecular, and Optical Physics*, 70(6), 1-9. https://doi.org/10.1103/PhysRevA.70.063410
- Physikd, F., Friedrich, B., & Herschbach, D. R. (1991). Atoms, Molecules Zeilschrilt and Clusters On the possibility of orienting rotationally cooled polar molecules in an electric field. *Molecules and Clusters*, 18(153), 153-161.
- Pickering, J. D., Shepperson, B., Hübschmann, B. A. K., Thorning, F., & Stapelfeldt, H. (2018). Alignment and Imaging of the CS2 Dimer Inside Helium Nanodroplets. *Physical Review Letters*, 120(11), 113202. https://doi.org/10.1103/PhysRevLett.120.113202
- Pullman, D. P., Friedrich, B., & Herschbach, D. R. (1990). Facile alignment of molecular rotation in supersonic beams. *The Journal of Chemical Physics*, 93(5), 3224-3236. https://doi.org/10.1063/1.458855
- Qin, M., & Zhu, X. (2017). Molecular orbital imaging for partially aligned molecules. *Optics and Laser Technology*, 87, 79-86. https://doi.org/10.1016/j.optlastec.2016.07.019
- Seideman, T. (1995). Rotational excitation and molecular alignment in intense laser fields. *The Journal of Chemical Physics*, 103(18), 7887-7896. https://doi.org/10.1063/1.470206
- Seideman, T. (1997). Molecular optics in an intense laser field: A route to nanoscale material design. *Physical Review A Atomic, Molecular, and Optical Physics*, 56(1), R17-R20. https://doi.org/10.1103/PhysRevA.56.R17
- Seideman, T., & Hamilton, E. (2005). Nonadiabatic Alignment by Intense Pulses. Concepts, Theory, and Directions. *Advances in Atomic, Molecular and Optical Physics*, *52*(05), 289-329. https://doi.org/10.1016/S1049-250X(05)52006-8
- Sinha, M. P., Caldwell, C. D., & Zare, R. N. (1974). Alignment of molecules in gaseous transport: Alkali dimers in supersonic nozzle beams. *The Journal of Chemical Physics*, 61(2), 491-502. https://doi.org/10.1063/1.1681923
- Sonoda, K., Iwasaki, A., Yamanouchi, K., & Hasegawa, H. (2018). Field-free molecular orientation of nonadiabatically aligned OCS. *Chemical Physics Letters*, 693, 114-120. https://doi.org/10.1016/j.cplett.2018.01.009
- Stapelfeldt, H., & Seideman, T. (2003). Colloquium: Aligning molecules with strong laser pulses. *Reviews of Modern Physics*, 75(2), 543-557. https://doi.org/10.1103/RevModPhys.75.543
- Tong, X. M., & Chu, S. I. (1997). Theoretical study of multiple high-order harmonic generation by intense ultrashort pulsed laser fields: A new generalized pseudospectral time-dependent method. *Chemical Physics*, 217(2-3 SPEC. ISS.), 119-130. https://doi.org/10.1016/s0301-0104(97)00063-3

- Tong, X. M., & Chu, S. I. (2000). Time-dependent approach to high-resolution spectroscopy and quantum dynamics of Rydberg atoms in crossed magnetic and electric fields. *Physical Review A Atomic, Molecular, and Optical Physics*, *61*(3), Article 031401. https://doi.org/10.1103/PhysRevA.61.031401
- Torres, R., De Nalda, R., & Marangos, J. P. (2005). Dynamics of laser-induced molecular alignment in the impulsive and adiabatic regimes: A direct comparison. *Physical Review A Atomic, Molecular, and Optical Physics*, 72(2), 1–8. https://doi.org/10.1103/PhysRevA.72.023420
- Villeneuve, D. M. (2018). Attosecond science. *Contemporary Physics*, *59*(1), 47-61. https://doi.org/10.1080/00107514.2017.1407093
- Watson, J. B., Sanpera, A., Lappas, D. G., Knight, P. L., & Burnett, K. (1997). Nonsequential double ionization of helium. *Physical Review Letters*, 78(10), 1884-1887. https://doi.org/10.1103/PhysRevLett.78.1884
- Yang, Z., & Zhou, X. (2006). Effect of Temperature on Alignment of N2 and O2 in Laser Field. *Acta Physico Chimica Sinica*, 22(8), 932-936. https://doi.org/10.1016/S1872-1508(06)60041-7

# MÔ PHỔNG SỰ ĐỊNH PHƯƠNG PHÂN TỬ PHI ĐOẠN NHIỆT Bùi Văn Nguyên<sup>1</sup>, Hoàng Trọng Đại Dương<sup>1, 2</sup>,

Trần Phúc Khang³, Triệu Đoan An¹, Phan Thị Ngọc Loan¹

<sup>1</sup>Trường Đại học Sư phạm Thành phố Hồ Chí Minh, Việt Nam <sup>2</sup>Trung tâm Đào tạo Hạt nhân - Viện Năng lượng nguyên tử Việt Nam, Hà Nội, Việt Nam <sup>3</sup>Viện Nghiên cứu Công nghệ New Jersey, Newark, Hoa Kì

\*Tác giả liên hệ: Hoàng Trọng Đại Dương – Email: hoangtrongdaiduong00@gmail.com Ngày nhận bài: 13-5-2024; Ngày nhận bài sửa: 14-02-2025; Ngày nhận đăng: 19-02-2025

#### TÓM TẮT

Gần đây, các kĩ thuật định hướng phân tử trở thành chủ đề quan tâm trong vật lí phân tử, vật lí trường mạnh, hóa học femto-giây và vật lí atto-giây. Định hướng phi đoạn nhiệt được ưa chuộng vì có thể sắp xếp phân tử trong không gian trong khoảng thời gian ngắn, dưới điều kiện không trường ngoài, tránh ảnh hưởng của laser đến hiện tượng vật lí hoặc hóa học. Do đó, việc phát triển chương trình mô phỏng định hướng phi đoạn nhiệt là cần thiết để kết quả số khớp với quan sát thực nghiệm. Các công cụ hiện có (Oppermann et al., 2012; Sonoda et al., 2018), hoặc chỉ áp dụng cho phân tử cụ thể, hoặc yêu cầu sửa đổi lớn. Chúng tôi cung cấp chương trình mô phỏng định hướng phi đoạn nhiệt cho các phân tử thẳng. Bài báo trình bày mô phỏng tiến hóa gói sóng quay phân tử bằng cách giải phương trình Schrödinger phụ thuộc thời gian và so sánh với các nghiên cứu đã công bố. Một thách thức là xác định tham số khai triển  $I_{max}$  tối ưu để vừa đảm bảo hội tụ nghiệm, vừa tiết kiệm tài nguyên tính toán. Chúng tôi đưa ra phương pháp chọn  $I_{max}$  có hệ thống. Chương trình được đánh giá với  $N_2$ ,  $CO_2$  và OCS ở nhiều xung laser và nhiệt độ khác nhau. Chương trình có sẵn tại: https://github.com/DuongDHoangTrong/HCMUE\_Alignment.

*Từ khóa:* tương tác laser-vật chất; phân tử thẳng; định phương phân tử phi đoạn nhiệt; bó sóng quay